Nonadiabatic tunnel ionization in strong circularly polarized laser fields: counterintuitive angular shifts in the photoelectron momentum distribution

Yang Li,[1] Pengfei Lan,[1,3] Hui Xie,[1] Mingrui He,[1] Xiaosong Zhu,[1] Qingbin Zhang,[1] and Peixiang Lu[1,2,*]

[1]*Wuhan National Laboratory for Optoelectronics and School of Physics, Huazhong University of Science and Technology, Wuhan 430074, China*

[2]*Laboratory of Optical Information Technology, Wuhan Institute of Technology, Wuhan 430073, China*

[3]*pengfeilan@hust.edu.cn*

[*]*lupeixiang@hust.edu.cn*

Abstract:
We perform time-dependent calculation of strong-field ionization of neon, initially prepared in $2p_{-1}$ and $2p_{+1}$ states, with intense near-circularly polarized laser pulses. By solving the three-dimensional time-dependent Schrödinger equation, we find clear different offset angles of the maximum in the photoelectron momentum distribution in the polarization plane of the laser pulses for the two states. We provide clear interpretation that this different angular offset is linked to the sign of the magnetic quantum number, thus it can be used to map out the orbital angular momentum of the initial state. Our results provide a potential tool for studying orbital symmetry in atomic and molecular systems.

OCIS codes: (320.0320) Ultrafast optics; (320.2250) Femtosecond phenomena; (320.7120) Ultrafast phenomena.

References and links

1. H. D. Cohen and U. Fano, "Interference in the photo-ionization of molecules," Phys. Rev. **150,** 30 (1966).
2. T. Zuo, A. D. Bandrauk, and P. B. Corkum, "Laser-induced electron diffraction: a new tool for probing ultrafast molecular dynamics," Chem. Phys. Lett. **259,** 313–320 (1996).
3. M. Meckel, D. Comtois, D. Zeidler, A. Staudte, D. Pavičić H. C.Bandulet, H. Pépin, J. C. Kieffer, R. Dörner, D. M. Villeneuve, and P. B. Corkum, "Laser-induced electron tunneling and diffraction," Science **320,** 1478–1482 (2008).
4. D. B. Milošević, G. G. Paulus, D. Bauer, and W. Becker, "Above-threshold ionization by few-cycle pulses," J. Phys. B **39,** R203 (2006).
5. W. Becker, F. Grasbon, R. Kopold, D. B. Milošević, G.G. Paulus, and H. Walther, "Above-threshold ionization: from classical features to quantum effects," Adv. At. Mol. Opt. Phys. **48,** 35–98 (2002).
6. D. B. Milošević and F. Ehlotzky, "Scattering and reaction processes in powerful laser fields," Adv. At. Mol. Opt. Phys. **49,** 373–532 (2003).
7. A. Becker and F. H. M. Faisal, "Intense-field many-body S-matrix theory," J. Phys. B **38,** R1–R56 (2005).
8. Y. Mairesse, A. de Bohan, L. J. Frasinski, H. Merdji, L. C. Dinu, P. Monchicourt, P. Breger, M. Kovačev, R. Taïzeb, B. Carré, H. G. Muller, P. Agostini, and P. Salères, "Attosecond synchronization of high-harmonic soft x-rays," Science **302,** 1540–1543 (2003).
9. P. Salières, A. Maquet, S. Haessler, J. Caillat, and R Taïeb, "Imaging orbitals with attosecond and Ångstörm resolutions: toward attochemistry?" Rep. Prog. Phys. **75,** 062401 (2012).

#249985 Received 11 Sep 2015; revised 19 Oct 2015; accepted 20 Oct 2015; published 26 Oct 2015

10. Y. Li, X. Zhu, P. Lan, Q. Zhang, M. Qin, and P. Lu, "Molecular-orbital tomography beyond the plane-wave approximation," Phys. Rev. A **89,** 045401 (2014).
11. J. Luo, Y. Li, Z. Wang, Q. Zhang, and P. Lu, "Ultra-short isolated attosecond emission in mid-infrared inhomogeneous fields without CEP stabilization," J. Phys. B: At. Mol. Opt. Phys. **46** 145602 (2013).
12. L. He, P. Lan, Q. Zhang, C. Zhai, F. Wang, W. Shi, and P. Lu, "Spectrally resolved spatiotemporal features of quantum paths in high-order-harmonic generation," Phys. Rev. A **92,** 043403 (2015).
13. A. Tong, Y. Zhou, and P. Lu, "Resolving subcycle electron emission in strong-field sequential double ionization," Opt. Express **23,** 15774 (2015).
14. Y. Zhou, C. Huang, Q. Liao, and P. Lu, "Classical simulations including electron correlations for sequential double ionization," Phys. Rev. Lett. **109,** 053004 (2012).
15. C. F. M. Faria and X. Liu, "Electroncelectron correlation in strong laser fields," J. Mod. Opt. **58,** 1076–1131 (2011).
16. I. Petersen, J. Henkel, and M. Lein, "Signatures of molecular orbital structure in lateral electron momentum distributions from strong-field ionization," Phys. Rev. Lett. **114,** 103004 (2015).
17. X. Zhu, Q. Zhang, W. Hong, P. Lu, and Z. Xu, "Molecular orbital imaging via above-threshold ionization with circularly polarized pulses," Opt. Express **19,** 13722 (2011).
18. L. Arissian, C. Smeenk, F. Turner, C. Trallero, A. V. Sokolov, D. M. Villeneuve, A. Staudte, and P. B. Corkum, "DirecttTest of laser tunneling with electron momentum imaging," Phys. Rev. Lett. **105,** 133002 (2010).
19. C. P. J. Martiny, M. Abu-samha, and L. B. Madsen, "Ionization of oriented targets by intense circularly polarized laser pulses: imprints of orbital angular nodes in the two-dimensional momentum distribution," Phys. Rev. A **81,** 063418 (2010).
20. T. Herath, L. Yan, S. K. Lee, and W. Li, "Strong-field ionization rate depends on the sign of the magnetic quantum number," Phys. Rev. Lett. **109,** 043004 (2012).
21. F. Mauger and A. D. Bandrauk, "Electronic dynamics and frequency effects in circularly polarized strong-field physics," J. Phys. B **47,** 191001 (2014).
22. I. Barth and O. Smirnova, "Nonadiabatic tunneling in circularly polarized laser fields: physical picture and calculations," Phys. Rev. A **84,** 063415 (2011).
23. I. Barth and O. Smirnova, "Nonadiabatic tunneling in circularly polarized laser fields. II. Derivation of formulas," Phys. Rev. A **87,** 013433 (2013).
24. I. Barth and M. Lein, "Numerical verification of the theory of nonadiabatic tunnel ionization in strong circularly polarized laser fields," J. Phys. B **47,** 204016 (2014).
25. D. Bauer and P. Koval, "QPROP: A Schrödinger-solver for intense laser-atom interaction," Comp. Phys. Comm. **174,** 396 (2006).
26. H. G. Muller, "Numerical simulation of high-order above-threshold-ionization enhancement in argon," Phys. Rev. A **60,** 1341 (1999).
27. A. N. Pfeiffer, C. Cirelli, M. Smolarski, D. Dimitrovski, M. Abu-samha, L. B. Madsen, and U. Keller, "Attoclock reveals natural coordinates of the laser-induced tunnelling current flow in atoms," Nat. Phys. **8,** 76 (2012).
28. K. J. Schafer and K. C. Kulander, "Energy analysis of time-dependent wave functions: Application to above-threshold ionization," Phys. Rev. A **42,** 5794 (1990).
29. C. P. J. Martiny, M. Abu-samha. and L. B. Madsen, "Counterintuitive angular shifts in the photoelectron momentum distribution for atoms in strong few-cycle circularly polarized laser pulses," J. Phys. B **42,** 161001 (2009).

1. Introduction

Photoionization of atoms and molecules has been studied since the early days of quantum mechanics with a perturbation manner [1]. Due to fast development of femtosecond laser pulses with field strengths equivalent to the field of the Coulomb interaction, strong-field ionization has become one of the fundamental highly nonlinear and nonperturbative processes in attosecond physics [2, 3]. In a linearly polarized laser field, the ionized electron can be driven back to the parent nucleus, resulting in various physical phenomena such as high-order above-threshold ionization due to electron rescattering [4–7], high harmonic generation [8–12] and non-sequential double ionization [13–15].

In the case of circularly polarized laser field, the electron born in the continuum is constantly driven away from the parent ion and can never travel back, which suppresses the rescattering effects as well as the interference between electron wavepackets launched at different times during the interaction with the driven pulses. Besides, the polarization plane of a circularly polarized laser field is two dimensional and thus the ellipticity provides an additional freedom for the electron motion. As a result, atomic or molecular photoionization exhibits some

#249985 Received 11 Sep 2015; revised 19 Oct 2015; accepted 20 Oct 2015; published 26 Oct 2015

new features that are absent in the case of linear polarization. For example, recent theoretical and experimental investigations have shown that the lateral widths of the electron momentum distribution at the tunneling exit is mapped onto the photoelectron momentum distributions (PMD) [16–18]. The symmetry property of the target atomic and molecular orbital has also been studied from the ionization signal in circularly polarized driving field. It has been shown that the use of circularly polarized field permits an more transparent interrogation of angular orbital structure of the targets and there are clear imprints of the angular nodes of the initial state in the two-dimensional PMD [19].

Another notable feature is the strong dependence of ionization probability on the sign of magnetic quantum number with respect to the rotation direction of the applied laser field [20]. The sign of the magnetic quantum number defines the direction of the electron "orbiting" the nucleus which can be clockwise or counterclockwise. Thus electron with different magnetic quantum number is co-rotating or counter-rotating relative to the laser field, which can be investigated in the rotating frame defined by the polarization direction of the laser field [21]. It has been shown that counter-rotating electrons which rotate against the circularly polarized laser fields can be more easily ionized that the co-rotating electrons [22–24].

All previous studies are focused on the dependence of ionization probability on the sign of magnetic quantum number. To the best of our knowledge, the PMDs of the co- and counter-rotating electrons have never been discussed. One notable exception is that Barth *et.al* have found different emission angles for valence p_{-1} and p_{+1} electrons in the evolution of electron probability density during the interaction with the laser field [24]. In their calculations, they presented radius-dependent positions corresponding to the angle where the electron probability density is maximal at different instants of time during the laser pulse and clear different emission angles for co- and counter-rotating electrons were found. However, they did not present observable which can be measured experimentally to extract the difference of the emission angles.

In this work, we focus on the difference of PMDs for co- and counter-rotating electrons. We calculated, by solving the three-dimensional time-dependent Schrödinger equation (TDSE), the PMDs for ionization of neon atom initially prepared in $2p_{-1}$, and $2p_{+1}$ states. The results show distinct effects of the orbital angular momentum of the initial orbital. Clear different offset angles of the maximum in PMD is found due to the difference of magnetic quantum number, indicating that strong-field ionization by circularly polarized laser fields directly probes the orbital angular momentum. Our results can be tested and have important implications using the angular attosecond streaking technique, which may make it possible to track the time-resolved angular momentum distribution in real time during a chemical reaction.

2. Results and discussions

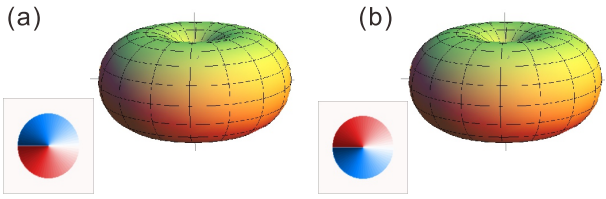

Fig. 1. The initial $2p_{-1}$ (a) and $2p_{+1}$ (b) orbitals of Neon atom. The insets show the phase of the two orbitals respectively. Electrons in $2p_{-1}$ state is counter-rotating and those in $2p_{+1}$ state is co-rotating for right circularly polarized laser field.

To this end, we numerically solve the velocity-gauge TDSE of neon atom initially prepared

#249985 Received 11 Sep 2015; revised 19 Oct 2015; accepted 20 Oct 2015; published 26 Oct 2015

in $2p_{-1}$ and $2p_{+1}$ state described in a single active electron (SAE) approximation [25] (atomic units are used unless stated otherwise):

$$i\frac{\partial}{\partial t}\Psi(\mathbf{r},t) = [\frac{\mathbf{p}^2}{2} + V(r) + \mathbf{A}(t)\cdot\mathbf{p}]\Psi(\mathbf{r},t). \quad (1)$$

In this equation, $V(r)$ is the Muller SAE potential [26] given by $V(r) = \frac{Z_c + Ae^{-Br} + (Z - Z_c - A)e^{-Cr}}{r}$, with $Z = 10.0$, $Z_c = 1.0$, $A = 2.74$, $B = 1.082$ and $C = 3.40$ to correctly reproduce the eigenenergy of $2p$ state. $\mathbf{A}(t)$ is vector potential of the laser field. Without imposing any physical restriction on the system, we assume that the laser is right near-circularly polarized in the (x,y) plane with ellipticity of $\varepsilon = 0.87$, in accordance with recent angular attosecond streaking experiments [27]. The x and y components can be expressed as $A_x(t) = -\varepsilon A_0 \sin^2(\frac{\pi t}{T})\sin(\omega t + \phi_{CEP})$ and $A_y(t) = A_0 \sin^2(\frac{\pi t}{T})\cos(\omega t + \phi_{CEP})$, where A_0 is the amplitude of the vector potential, ω, T and ϕ_{CEP} are the frequency, total duration and CEP of the laser field,respectively. In our calculation, $\omega = 0.057$ a.u. conforms with Ti:sapphire 800 nm laser pulse with total duration of 10 optical cycle and intensity of $1.4 \times 10^{14}\mathrm{W/cm^2}$. ϕ_{CEP} is set as 0. Figure 1 presents the $2p_{-1}$ and $2p_{+1}$ valence states of Neon atom. For right polarized laser field, the electron of $2p_{-1}$ state is counter-rotating with respect to the polarization direction of the laser field and the $2p_{+1}$ state is co-rotating.

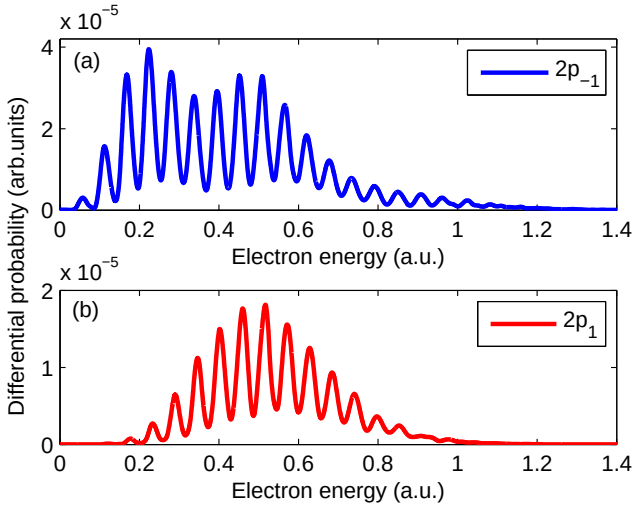

Fig. 2. Photoelectron energy spectra of neon starting from the valence $2p_{-1}$ (a) and $2p_{+1}$ (b) orbitals for 800 nm right near-circularly polarized laser field.

Firstly, we calculate the integrated energy spectra of the ionized electrons using the energy window operator technique, which is introduced by Schafer and Kulander [28]. The window operator is defined as $W(E,k,\gamma) = \gamma^{2k}/[(H_0 - E)^{2k} + \gamma^{2k}]$, with $H_0 = \mathbf{p}^2/2 + V(r)$. γ is the energy width and k is the integer order of the window operator. Here we choose the parameters $\gamma = 0.05$ and $k = 2$. The electron energy spectra of $2p_{-1}$ and $2p_{+1}$ are shown in Fig. 2(a) and 2(b), respectively. One clearly identifies conspicuous above-threshold ionization peaks which are separated by one-photon energy $\hbar\omega$ in both spectra. On the other hand, an important feature one can find from the integrated energy spectra is that the strong-field ionization rate of the $2p_{-1}$ orbital is about 2 times higher than that of $2p_{+1}$ in the right near-circularly polarized light field. This point is consistent with previous theoretical and experimental investigations [20,24]. An intuitive physical interpretation can be provided to explain the magnetic quantum number

#249985 Received 11 Sep 2015; revised 19 Oct 2015; accepted 20 Oct 2015; published 26 Oct 2015

dependence of the strong-field ionization rate by circularly polarized laser field. In a laser field, the Coulomb potential of the atom is suppressed, such that the electron can tunnel out from the barrier. For circularly polarized laser, the suppressed Coulomb barrier is rotating with the same frequency of the laser. For co- and counter-rotating electrons with opposite magnetic quantum number, moving the system into a frame rotating with the laser field, the frequency of the counter-rotating electrons meeting the suppressed Coulomb barrier is higher than that of the co-rotating electrons. As a result, the strong field ionization rate of $m = -1$ is higher. Besides the different ionization rates of the $2p_{+1}$ and $2p_{-1}$ states, one can clearly find that there are energy shifts in the photoelectron energy spectra comparing Fig. 2(a) and 2(b). The energy shift can also been viewed in photoelectron momentum spectra as radial momentum shifts (see Fig. 3(a) and 3(b)). We would point out that energy shifts and radial momentum shifts of the photoelectron spectra are in accordance with the analytical results of Ref. [23] (see Fig. 3 of Ref. [23]).

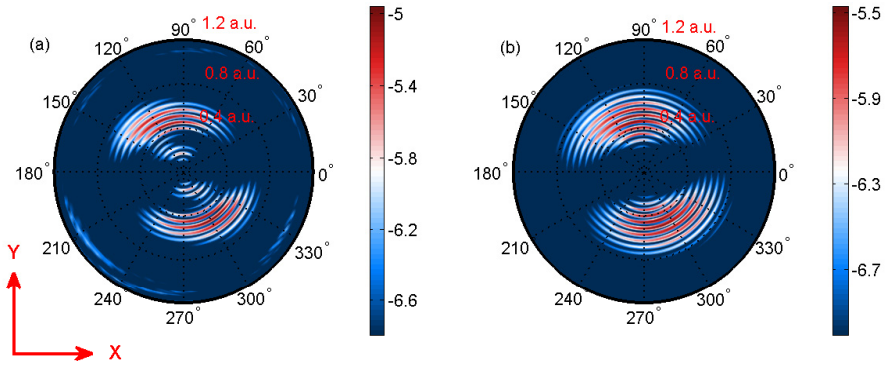

Fig. 3. Angle- and momentum-resolved photoelectron spectra produced by the strong field ionization of neon using 800 nm right near-circularly polarized laser field starting from the valence $2p_{-1}$ (a) and $2p_{+1}$ (b) orbitals. The inset shows the axis of the laser field, The y direction indicate the peak direction of the vector potential, which is the axis of zero offset angle.

In what follows, we focus on the photoelectron momentum distributions for the neon atom initially prepared in $2p_{-1}$ and $2p_{+1}$ states. Distributions are calculated on the polarization xy plane with a dense momenta grid using polar coordinates, as shown in Fig. 3. In both two cases, one observes two nearly symmetric peaks in the PMDs. Each one contains well resolved rings corresponding above threshold ionization peaks. As we use near-circularly polarized laser fields with ellipticity of 0.87, the peak direction of the electric field envelope is easily determined. The peak of the electric field envelope coincides with the orientation of the major axis of the polarization ellipse, ensuring the maximum value of the vector potential. One can see from Fig. 3(a) and 3(b) that the maximum of the PMDs for $2p_{-1}$ and $2p_{+1}$ orbitals show different offset angles with respect to the major axis of polarization ellipse. The offset angle for the $2p_{-1}$ orbital is larger than it is for the $2p_{+1}$ orbital. In order to find the maximum of the angular distributions, we integrate the momentum distributions over radial direction and analyze the one-dimensional angular distributions, as presented in Fig. 4. The resulting angular distributions show noticeable offset angles relative to y axis. The offset are 19.6° for $2p_{+1}$ state and 32.1° for $2p_{-1}$ state. Note that the offset angles also exists for m=0 state because of the influence of the Coulomb potential, which has been proved both theoretically and experimentally. Quantum mechanically, the $m = 0$ orbital can be viewed as a superposition of $m = -1$ and $m = 1$ orbitals. We expect the mean

#249985 Received 11 Sep 2015; revised 19 Oct 2015; accepted 20 Oct 2015; published 26 Oct 2015

offset angle of $2p_{-1}$ and $2p_{+1}$ orbitals is comparable with the offset of $m = 0$ state.

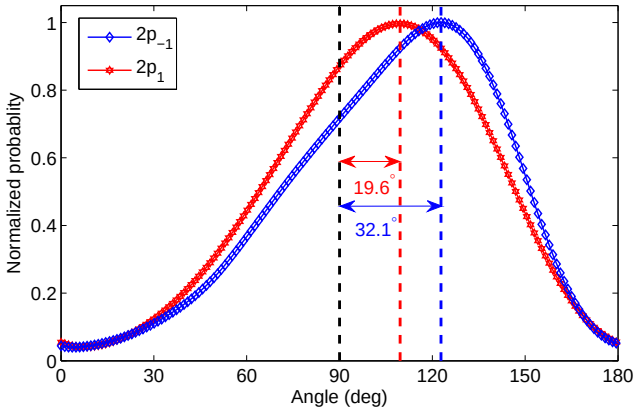

Fig. 4. The radial integrated photoelectron distributions as the functions of the angle for $2p_{-1}$ (blue curves) and $2p_{+1}$ (red curves) orbitals of neon.

Next, we will show that the different offset angle for $2p_{-1}$ and $2p_{+1}$ orbitals manifests itself in the ionization probability of different magnetic quantum numbers [29]. For laser pulse polarized in the x-y plane, as considered in present work, the symmetry of the atom is broken, such that the angular momentum projection m is no longer conserved, i.e., $[\hat{H}, \hat{L}_z] = i(\hat{p}_x A_y - \hat{p}_y A_x) \neq 0$ during the laser pulse for $\hat{H} = \mathbf{p}^2/2 + V(r) + \mathbf{A}(t) \cdot \mathbf{p}$. It means that $\langle \hat{L}_z \rangle = \langle \Psi | \hat{L}_z | \Psi \rangle$ changes during interaction with the laser pulse according the Ehrenfest theorem, until it becomes constant after the laser pulse. We calculated the probability distribution as a function of magnetic quantum number for $2p_{-1}$ and $2p_{+1}$ orbitals from the ionized part of the electron wave packet, as presented in Figs. 5(a) and 5(b). The $m = \pm 1$ component is removed. One can see that for $2p_{-1}$ state the probability distribution peaks around $m \cong 20$ while for $2p_{+1}$ state the peaks shift to $m \cong 30$. The difference of the probability distribution as a function of magnetic quantum number causes the different offset angle of the angle-resolved photoelectron spectra, which can also be interpreted by a more transparent way. The counter-rotating and co-rotating electrons, corresponding to p- and p+ orbitals respectively, have different initial orthogonal velocities with respect to the tunneling direction. The counter-rotating electron is "slower". Instead, the co-rotating electron has higher lateral momentum. As a result, under the influence of the laser field and the core potential, the counter-rotating electron strongly interacts with the Coulomb potential due to its lower momentum. Whereas the co-rotating electron moves away faster. Therefore it is less affected by the Coulomb potential. This leads to the offset angle of p- orbital is larger than that of p+ orbitals. Therefore, the PMD can be a promising tool to study the laser populating process during the interaction with atoms and molecules.

3. Conclusion

In summary, using 3-dimensional quantum mechanical model, we studied the strong field ionization of neon atom stating from initial $2p_{-1}$ and $2p_{+1}$ states with opposite magnetic quantum number. The resulting photoelectron momentum distributions of the two states show clear different angle offsets of the maximum, which has never been reported before to the best of our knowledge. By calculating the laser populating probability of specific magnetic quantum number of the ionized wave packet after the laser pulse, we pointed that the different offset angles were linked to the difference of the probability distribution as a function of magnetic quantum

#249985 Received 11 Sep 2015; revised 19 Oct 2015; accepted 20 Oct 2015; published 26 Oct 2015

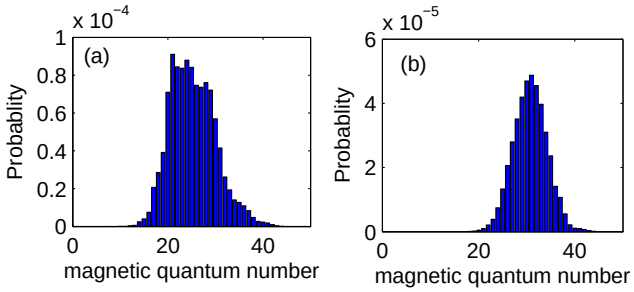

Fig. 5. The probability distribution for different magnetic quantum number after the laser pulse from the ionized part of the electron wave packet: (a) for $2p_{-1}$ orbital and (b) for $2p_1$ orbital.

number.

Acknowledgment

We would like to thank Prof. Dieter Bauer for helpful discussions with the QPROP package. This work was supported by the National Natural Science Foundation of China under Grants No. 11234004, No. 11404123 and No. 61275126, the 973 Program of China under Grant No. 2011CB808103. Numerical simulations presented in this paper were carried out using the High Performance Computing Center experimental testbed in SCTS/CGCL (see http://grid.hust.edu.cn/hpcc).

#249985 Received 11 Sep 2015; revised 19 Oct 2015; accepted 20 Oct 2015; published 26 Oct 2015